IAEA SYMPOSIUM ON MEDICAL RADIONUCLIDE IMAGING

October 25-29, 1976
Los Angeles, California, U.S.A.

IAEA-SM-210/123

DEVELOPMENT OF POSITRON EMITTING RADIONUCLIDES FOR IMAGING WITH IMPROVED POSITRON DETECTORS

Y. Yano
Donner Laboratory, University of California, Berkeley U.S.A.

Abstract

Recent advances in positron cameras and positron ring detectors for transverse section reconstruction have created renewed interest in positron emitting radionuclides. This paper reports on: 1) generator produced ^{82}Rb; 2) cyclotron produced ^{62}Zn; and 3) reactor produced ^{64}Cu.

Investigation of the ^{82}Sr (25 d)-^{82}Rb (75 s) generator determined the elution characteristics for Bio-Rex 70, a weakly acidic carboxylic cation exchanger, using 2% NaCl as the eluent. The yield of ^{82}Rb and the break-through of ^{82}Sr were determined for newly prepared columns and for long term elution conditions. Spallation produced ^{82}Sr was used to charge a compact ^{82}Rb generator to obtain multi-millicurie amounts of ^{82}Rb for myocardial imaging.

Zinc accumulates in the islet cells of the pancreas and in the prostate. Zinc-62 was produced by protons on Cu foil and separated by column chromatography. Zinc-62 was administered as the amino acid chelates and as the $ZnCl_2$ to tumor and normal animals. Tissue distribution was determined for various times after intravenous injection. Pancreas-liver images of ^{62}Zn-histidine uptake were obtained in animals with the gamma camera and the liver uptake of ^{99m}Tc sulfur colloid was computer subtracted to image the pancreas alone. The positron camera imaged uptake of ^{62}Zn-histidine in the prostate of a dog at 20 h.

^{64}Cu was chelated to asparagine, a requirement of leukemic cells, and administered to lymphoma mice. Uptake in tumor and various tissues was determined and compared with the uptake of ^{67}Ga citrate under the same conditions. ^{64}Cu-asparagine had better tumor to soft tissue ratios than ^{67}Ga-citrate.

Recent advances in positron cameras and the development of positron ring detectors for transverse section reconstruction tomography [1-6] have created renewed interest in positron emitting radionuclides which are most conveniently obtained from generators such as ^{62}Zn-^{62}Cu, ^{68}Ge-^{68}Ga, ^{82}Sr-^{82}Rb, or ^{122}Xe-^{122}I. Alternatively, they can be produced primarily by accelerator irradiation or, as in the case of ^{64}Cu, by thermal neutron irradiation. This paper reports on three recent developments with positron emitting radionuclides: 1) generator produced ^{82}Rb for myocardial imaging; 2) cyclotron produced ^{62}Zn for pancreas and prostate imaging; and 3) reactor produced ^{64}Cu for localization in transplanted lymphomas in mice.

^{82}Sr/^{82}Rb Generator

Rubidium-82, $T_{1/2}$ 75 s, is conveniently available from a 25 d ^{82}Sr parent. The short half-life ^{82}Rb decays 96% by positron emission to provide a high flux of positron annihilation photons without a high radiation dose to the patient. Serial scans can be done every 5-10 min to image the myocardium which extracts the ^{82}Rb.

The use of cyclotron or spallation produced ^{82}Sr in the development of a Bio-Rex 70 (weakly-acidic carboxylic cation exchange resin) generator has shown the value of this system [7-8]. A compact version of the ^{82}Rb generator was developed and evaluated for myocardial imaging with the multi-crystal positron camera [9-10]. Other investigators have used the chelating ion exchange resin Chelex-100 in another type of ^{82}Sr-^{82}Rb generator [11]. This is an evaluation of the elution characteristics of the ion exchange resin Bio-Rex 70 and the effect of long term elutions on the breakthrough of ^{82}Sr from the resin column.

The ^{82}Sr was produced by spallation reaction with medium energy protons on molybdenum target and radiochemically separated by the method previously reported [12]. Considerable amounts of ^{85}Sr were also produced. About eight weeks after the Mo target irradiation the ratio of ^{85}Sr to ^{82}Sr was 2.3.

The processed ^{82}Sr solution was used to charge Bio-Rex 70 columns for loading into the compact generator shown in Fig. 1. The *Sr ($^{82+85}$Sr) in HCl solution was adjusted to pH 8.0 with NH_4OH for the Bio-Rex 70 resin column. A tenfold dilution was made with sterile distilled water, and the *Sr solution was passed through the specially-machined, stainless-steel columns shown in Fig. 2. The design of the column permits rapid connection into the compact generator. The resin volumes were 3.92 ml in the main column and 0.68 ml in the trapping column. The total resin volume of 4.6 ml gave a reasonable ^{82}Rb yield in an injectable volume with low breakthrough of radiostrontium. The useful life of the generator was prolonged by simply replacing the trapping column with a freshly charged resin unit whenever the Sr breakthrough became excessive (> 0.5 μCi).

Elutions of ^{82}Rb from the Bio-Rex 70 generator were done with 2% NaCl solution, adjusted to pH 8.0, at a flow rate of 0.5-1.0 ml/s.

The retention of *Sr by Bio-Rex 70 was > 99% as a result of the column-loading procedure. The elution yield of ^{82}Rb and the *Sr breakthrough for a typical Bio-Rex 70 column are shown in Table I. The ^{82}Rb yield was about 70% with 20 ml of 2% NaCl. The leakage of *Sr activity was about 0.0004 μCi per 20-ml elution. The breakthrough of *Sr (μCi Sr eluate/μCi Sr resin col) was 7×10^{-9} or a separation factor of 1×10^{8} (fraction ^{82}Rb/breakthrough). Long-term elution data plotted in Fig. 3 shows the *Sr breakthrough has increased to 0.02 μCi by 0.9 liter and to 0.3 μCi after passage of 1.4 liters (70 elutions) through the column over a period of about one month.

The radiation dose from 0.1 μCi of ^{82}Sr is 40 mR to total bone, 38 mR to red marrow and 4 mR total body [13]. A comparable dose of ^{85}Sr delivers a radiation dose of 4 mR to total bone, 3 mR to red marrow and 1.4 mR total body. The radiation dose from 10 mCi of ^{82}Rb is primarily to the kidneys which receive 740 mR.

The favorable elution characteristics of the Bio-Rex 70 ion-exchange chromatographic separation system enclosed in a readily transportable generator is a potential asset for myocardial and blood-flow imaging when it is used in conjunction with a fast-response and tomographic positron imaging system.

Zinc-62 for Pancreas and Prostate

Zinc is known to accumulate in the islet cells of the pancreas and in the prostate, possibly as a metalloenzyme [14,15]. Zinc also forms chelates with amino acids. A number of studies have been done with ^{65}Zn, ^{69m}Zn and ^{62}Zn in animals and humans to image the prostate and to determine the in vivo distribution of zinc radionuclides usually in the form of $ZnCl_2$ [16-23].

Zinc-62, $T_{½}$ 9.3 h, decays 80% by EC and 20% by β+ (660 keV_{max}) emission to the 9.8 min ^{62}Cu which decays 97% by β+ (2.91 MeV_{max}) emission and 2% by EC to stable ^{62}Ni. In addition to the 511 keV β+ annihilation gamma-rays, the ^{62}Zn has 590 keV (22%) and 42 keV (20%) gamma-rays, the ^{62}Cu daughter has gamma-rays of 511 keV (195%), 880 keV (0.3%) and 1.19 MeV (5%).

Zinc-62 was produced by irradiating 0.13 mm thick copper foil with 30 MeV protons at the Lawrence Berkeley Laboratory's 88 inch cyclotron. The average beam current was 10-15 μA with an integrated beam of 25 μAh. The production yield was about 1.0 mCi/μAh at the end of the irradiation.

The Cu target foil was brought into solution with a minimum volume of 1:1 HNO_3 and evaporated to near dryness. Concentrated HCl acid was added and the solution was again taken to near dryness. The residue of $CuCl_2$-$^{62}ZnCl_2$ was brought into solution with 2.5 M HCl acid and passed through a 1 cm dia x 10 cm high column of AG 1 x 8, 100-200 mesh, anion exchange resin which had been pre-washed with 2.5 M HCl.

The resin column was washed with 50 ml of 2.5 M HCl to remove the Cu. The ^{62}Zn remaining on the resin column was then eluted with 50 ml of sterile water and collected in 10 ml fractions. Twenty mg of amino acid were added to the $^{62}ZnCl_2$ in a 10 ml H_2O fraction. The pH was adjusted to 5.5-6.0 with dilute $NaHCO_3$ and the solution was passed through a 0.22 μm membrane filter. More than 95% of the ^{62}Zn activity was in the filtrate.

Five amino acids: alanine, arginine, cysteine, histidine and tryptophan (Caliochem) as the hydrochloride, were used as the ^{62}Zn-amino acid chelates in animal studies with rats, dogs and monkeys. In addition, $^{62}ZnCl_2$ at pH 2-3 was used in similar studies to compare the chelation effect to the colloid in reducing liver uptake relative to pancreas uptake.

Uptake of the various amino acid chelates of ^{62}Zn and $^{62}ZnCl_2$ in male Sprague-Dawley rats (250-350 g) 1.5 h and 20 h post injection for pancreas and prostate are shown in Table II. The uptake ratio of pancreas to liver was 0.86 for histidine, 0.92 for the chloride and 1.1 for arginine; the prostate uptake was greatest for histidine at 1.19% dose/g compared to

1.06%/g for tryptophan and 0.94%/g for chloride.

The results of the uptake of ^{62}Zn-histidine in rats with time indicates the maximum uptake in pancreas was reached at 1.5 h post injection while the maximum uptake in liver was at 0.7 h. For the prostate the highest uptake occurred at 20 h.

There was a better prostate to muscle ratio of 9.6 for the ^{62}Zn-cysteine chelate compared to 4.8 for histidine. However, the % dose/gm uptake of histidine (1.19 ± 0.19) in the prostate is greater than ^{62}Zn-cysteine. Although the pancreas to liver ratio of 1.1 for arginine was greater than 0.91 for histidine, neither ratio was significantly improved over that obtained with the ionic ^{62}Zn at 0.92.

Our dog uptake studies with ^{62}Zn-histidine give a pancreas to liver ratio of 0.61, whereas studies with "carrier" ^{69m}Zn yielded a lower ratio of 0.34 for $^{69m}ZnCl_2$.

The blood clearance curve for whole blood of dog (Figure 4) demonstrated two components with half-times of 3.5 min and 39 min. About 5% of the injected dose was in whole blood 70 min after intravenous injection.

Sufficient activity accumulated in the prostate of the beagle dog (Figure 5) to allow good visualization of the prostate 17 h after intravenous injection of 200 μCi ^{62}Zn-histidine. Table III shows the relative concentrations of ^{62}Zn-histidine determined by counting individual organs. The pancreas/liver ratios were 0.6 and 1.1 at 2 and 24 h post injection respectively. The prostate/gut ratios were 1.0 and 1.9 for the 2 and 24 h periods respectively. The liver and pancreas have the highest concentration of ^{62}Zn-histidine followed by prostate, kidney and gut.

A subhuman primate study shows uptake in the pancreas (Figure 6) in studies done at 1 h after i.v. injection of 700 μCi of ^{62}Zn-histidine. The pancreas image was confirmed by subtraction studies in which ^{99m}Tc sulfur colloid was used to remove the liver image. This study was compared to a standard ^{75}Se-methionine and ^{99m}Tc sulfur colloid study in the same animal.

The radiation dose for ^{62}Zn has been calculated to be 0.8 rads/mCi whole body, 12 rads/mCi to each of liver, pancreas and prostate and 6 rads/mCi to kidneys in agreement with Chisholm et al. [23].

We expect the "carrier" effect to be an important factor on the biological distribution of radioactive Zn tracers. These preliminary studies indicate a potential use for ^{62}Zn possibly as a histidine chelate or with other amino acids, for selective imaging of pancreas and prostate.

The specific activity of ^{62}Zn-amino acid chelate in the prostate relative to pelvic organs is adequate for quantitative in vivo uptake studies using positron transaxial tomographic devices. The similarity in uptake between liver and pancreas will necessitate dual isotope studies which can be done by following a ^{62}Zn-amino acid study with a ^{68}Ga colloid or ^{99m}Tc-sulfur colloid study.

^{64}Cu-Asparagine

Asparagine is a requirement of lymphoblastic leukemic cells as evidenced by the chemotherapeutic effect of asparaginase [24]. ^{64}Cu-asparagine (log

K 14.9) was administered to tumor bearing mice. Copper-64 ($T_{1/2}$ 12.8 h, decaying by 19% β^+, 38% β^- and 43% electron capture) was produced by irradiating 6 mg of Cu wire (9.5×10^{-2} mM) for 2 h in 3.2×10^{13} n/cm^2·s at the TRIGA Reactor (University of California, Berkeley) to yield about 8 mCi of ^{64}Cu. The Cu wire was dissolved in HNO_3 and the pH adjusted to 4.5 with dilute NaOH. Thirty mg of asparagine monohydrate (Calbiochem), 2×10^{-1} mM, in 2 ml of sterile H_2O were added to the ^{64}Cu and filtered through a 0.22 μm membrane filter.

The ^{64}Cu-asparagine in a volume of 0.15 ml was given by tail vein to A/HeJ mice two weeks after subcutaneous transplantation of L-2 lymphoma cells. The uptake in tumor and tissue was determined at 3 h and 24 h after intravenous injection and compared with ^{67}Ga citrate uptake under the same conditions. These results are shown in Tables IV and V. The uptakes of ^{64}Cu-asparagine and ^{67}Ga-citrate at 3 h were 3.15%/g and 4.93%/g respectively in tumor and 4.75%/g and 27.1%/g respectively in blood, or a tumor/blood ratio of 0.93 for ^{64}Cu-asparagine and 0.12 for ^{67}Ga-citrate; at 22 h the uptakes of ^{64}Cu and ^{68}Ga were 2.30%/g and 3.96%/g respectively in tumor and 0.98%/g and 3.89%/g respectively in blood, or a tumor/blood ratio of 2.3 for ^{64}Cu and 1.4 for ^{68}Ga.

The tissue distribution of ^{64}Cu-asparagine, due to its faster clearance from blood and soft tissues, appears to be more favorable than ^{67}Ga-citrate for earlier imaging times. Improved positron imaging systems may prove to be an advantage in the localization of lymphomas.

Conclusions

Positron emitting radionuclides can be applied to nuclear medicine imaging procedures without the need for an on site cyclotron by utilizing generators or by using intermediate half-life (8-10 h) radionuclides which can be transported from a cyclotron or reactor production site. However, biochemically significant organic compounds must be labeled with 20 m ^{11}C or 9.9 m ^{13}N produced by an on-site cyclotron.

REFERENCES

[1] BURNHAM, C.A., BROWNELL, G.L., A multi-crystal positron camera, IEEE Trans. Nucl. Sci. 19 (1972) 201.

[2] MUEHLLEHNER, G., Positron camera with extended counting rate capability, J. Nucl. Med. 16 (1975) 653.

[3] PHELPS, M.E., et al., "Transaxial Remission Reconstruction Tomography: Coincidence Detection of Positron Emitting Radionuclides", in Noninvasive Brain Imaging, Computed Tomography and Radionuclides. (DeBLANC, H.J., Jr., SORENSON, J.A., Eds), Society of Nuclear Medicine, New York (1975) 87.

[4] LIM, C.B., et al., Initial characterization of a multiwire proportional chamber positron camera, IEEE Trans. Nucl. Sci. 22 (1975) 388.

[5] DERENZO, S.E., ZAKLAD, H., BUDINGER, T.F., Analytical study of a high-resolution positron ring detector system for transaxial reconstruction tomography, J. Nucl. Med. 16 (1975) 1166.

[6] CHO, Z.H., CHAN, J.K., ERIKSSON, L., Circular ring transverse axial positron camera for three-dimensional reconstruction of radionuclide distribution, IEEE Trans. Nucl. Sci. 23 (1976) 613.

[7] YANO, Y., ANGER, H.O., Visualization of heart and kidneys in animals with ultrashort-lived ^{82}Rb and the positron camera, Nucl. Med. 9 (1968) 412.

[8] YANO, Y., BUDINGER, T.F., CHU, P., GRANT, P.M., OGARD, A.E., O'BRIEN, H.A., HOOP, B., Jr.,Evaluation of Rubidium-82 generators for imaging studies, J. Nucl. Med. 17 (1976) 536.

[9] BUDINGER, T.F., YANO, Y., HOOP, B., Jr.,A comparison of ^{82}Rb and ^{13}NH$_3$ for myocardial perfusion scintigraphy, J. Nucl. Med. 16 (1975) 429.

[10] HOOP, B., Jr.,BEH, R.A., et al., Myocardial positron scintigraphy with short-lived ^{82}Rb, IEEE Trans. Nucl. Sci. 23 (1976) 584.

[11] GRANT, P.M., ERDAL, B.R., O'BRIEN, H.A., A ^{82}Sr-^{82}Rb isotope generator for use in nuclear medicine, J. Nucl. Med. 16 (1975) 300.

[12] GRANT, P.M., KAHN, M., O'BRIEN, H.A., The isolation of ^{82}Sr from 200 to 600 meV proton-irradiated Mo targets for biomedical applications. J. Inorg. Nucl. Chem. 37 (1975) 413.

[13] HOOP, B., Jr., MGH IND 11821.

[14] MAWSON, C.A., FISHER, M.I., The occurrence of zinc in the human prostate gland, Canad. J. Med. Sci. 29 (1951) 336.

[15] MIKAC-DEVIC, D., Methodology of zinc determinations and the role of zinc in biochemical processes, Adv. Clin. Chem. 13 (1970) 271.

[16] SIEGEL, E., GRAIG, F.A., CRYSTAL, M.M., AND SIEGEL, E.P., Distribution of ^{65}Zn in the prostate and organs of man. The Br. J. of Cancer. 15 (1961) 647.

[17] SPENCER, H., ROSOFF, B., LEWIN, I., SAMACHSON, J., Studies of zinc-65 metabolism in man. In Zinc Metabolism,(PRASAD, A., Ed.) Charles C. Thomas, Springfield, Ill., (1966) 339-362.

[18] JOHNSTON, G., WADE, M.D., et al, ^{65}Zn and ^{69m}Zn studies in the dog, monkey and man. J. Surg. Research. 8 (1970) 231-238.

[19] BUDDY, K., EAST, B.W., KING, P.C. et al, Preliminary studies of zinc metabolism in carcinoma of the prostate gland. British J. Urology. 42 (1970) 475.

[20] GOLD, F.M. and LORGER, S.A., Radioisotope ^{69m}Zn chloride prostate gland scan. Invest. Urology. 8 (1970) 231

[21] GREENLAW, R.H., STRAIN, W.H., CALLEAR, T.E., OUBILLER, L.D., and STRAIN, S.C., Experimental studies for scintillation scanning of the pancreas. J. Nucl. Med. 3 (1962) 47.

[22] WAKELEY, J.C.N., MOFFATT, B., CROOK, A., and MALLARD, J.R., The distribution and radiation dosimetry of zinc-65 in the rat. Intl. J. Appl. Rad. and isotopes. 7 (1960) 225.

[23] CHISHOLM, G.D., SHORT, M.D., CHANADIAN, R., McRAE, C.U., and GLASS, H.I., Radiozinc uptake and scinti-scanning in prostatic disease. J. Nucl. Med. 15 (1974) 739.

[24] ALEXANDER, P., "Anti-leukaemic action of l-asparaginase", Fundamentals of Biochemical Pharmacology, (BACQ, Z.M., Ed.) Pergamon Press, Oxford, (1971) 517.

TABLE I. ELUTION YIELD OF ^{82}Rb AND BREAKTHROUGH OF ^{a}Sr FROM BIO-REX 70 COLUMN

Elution Number	Yield of ^{82}Rb mCi	%	^{a}Sr Leakage μCi	^{b}Break-through	^{c}Separation Factor
$^{d}5$	7.03	97.1	0.0012	1.9×10^{-8}	5.2×10^{7}
6	5.56	76.8	0.0003	[illegible].9 x 10^{-9}	1.5×10^{8}
7	5.70	78.7	0.0004	6.9×10^{-9}	1.1×10^{8}

a) ^{82}Sr and ^{85}Sr
b) Breakthrough = ^{a}Sr eluate/^{a}Sr resin (6.8 mCi ^{82}Sr + 53.3 mCi ^{85}Sr for Chelex and 7.2 mCi ^{82}Sr + 55.6 mCi ^{85}Sr for Bio-Rex)
c) Separation Factor = Fraction of ^{82}Rb x breakthrough^{-1}
d) Elutions with 2% NaCl, pH 8.0 (20 ml)

TABLE II

Uptake of ^{62}Zn-amino acid and chloride in normal rats with time after i.v. injection

Percent injected dose per gram ± s.d.*+

	(t-hr)	Blood	Liver	Kidneys	Spleen	Pancreas	Prostate	Muscle	Femur	Pancreas/Liver	Prostate/Muscle
Alanine	1.5hr	0.22±0.07	2.74±1.44	2.84±0.99	1.35±0.35	1.51±0.35	0.40±0.10	0.12±0.07	0.52±0.41	0.55	3.33
	20hr	0.14±0.02	1.26±0.20	0.91±0.15	1.10±0.17	0.90±0.35	1.24±——	0.22±0.08	0.89±0.47	0.71	5.63
Cysteine	1.5hr	0.21±0.03	2.20±0.14	2.41±0.52	1.27±0.20	1.59±0.10	0.66±0.20	0.08±0.01	0.29±0.02	0.72	8.25
	20hr	0.10±0.01	0.91±0.15	0.74±0.13	0.74±0.06	0.43±0.14	1.05±0.36	0.11±0.01	0.35±0.04	0.47	9.55
Histidine	0.7hr	0.42±0.14	3.73±0.23	3.35±0.54	1.74±0.07	2.20±0.32	0.52±0.08	0.17±0.01	0.58±0.02	0.59	3.06
	1.5hr	0.30±0.02	2.71±0.34	3.08±0.30	1.45±0.43	2.32±0.17	0.71±0.20	0.19±0.01	0.71±0.07	0.86	3.74
	20hr	0.19±0.02	1.40±0.17	1.30±0.19	1.29±0.12	1.07±0.13	1.19±0.15	0.25±0.07	1.14±0.70	0.76	4.76
Tryptophan	1.5hr	0.21±0.02	2.11±0.07	2.29±0.19	1.22±0.13	1.58±0.57	0.40±0.31	0.07±0.05	0.56±0.14	0.75	5.71
	20hr	0.15±0.05	1.19±0.25	1.23±0.69	1.10±0.44	0.91±0.27	1.06±0.63	0.18±0.06	0.71±0.20	0.76	5.89
Arginine	1.5hr	0.19±0.06	2.29±0.29	2.43±0.59	1.52±0.31	2.44±0.69	0.64±0.31	0.14±0.02	0.61±0.13	1.07	4.57
	20hr	0.12±0.00	1.03±0.12	0.83±0.08	0.93±0.04	0.66±0.10	0.93±0.43	0.16±0.01	0.83±0.08	0.64	5.61
Chloride	0.7hr	0.39±0.05	4.07±0.20	3.40±0.17	1.76±0.07	2.26±0.37	0.46±0.02	0.18±0.01	0.67±0.05	0.55	2.56
	1.5hr	0.46±0.18	2.66±0.24	3.44±0.14	1.78±0.19	2.46±0.42	0.57±0.15	0.19±0.00	0.80±0.01	0.92	3.00
	20hr	0.15±0.03	1.48±0.43	1.10±0.26	1.13±0.29	1.17±0.17	0.94±0.20	0.20±0.07	0.89±0.52	0.79	4.70

* Values are the mean of 3-4 animals.

\+ Log K: Alanine 9.5; Arginine 7.3; Cysteine 16.6; Histidine 12.9; and tryptophan 9.3 (Ref.18 & 19)

TABLE III

^{62}Zn - histidine distribution

	12.3Kg Beagle Male AFTER 2 HOURS		11.8Kg Beagle Male AFTER 24 HOURS	
	% activity per organ	% activity per gram (× 10^2)	% activity per organ	% activity per gram (× 10^2)
PANCREAS	1.7	4.6	2.7	9.3
LIVER	43.1	7.5	32.3	8.7
PROSTATE	0.2	2.7	0.4	6.2
KIDNEYS	3.5	3.3	2.2	2.6
GUT	14.7	2.8	16.0	3.5
COLON	0.8	0.4	4.0	4.6
STOMACH	17.5	1.2	2.0	1.7
HEART	1.4	7.3	1.6	1.2
LUNGS	1.0	0.6	1.2	1.1
SPLEEN	1.0	2.0	0.9	0.6
CARCUS	27.0	0.3	37.0	0.4
TESTES	.07	0.4	---	---
PANCREAS/LIVER		0.6		1.1
PROSTATE/GUT		1.0		1.8

Table IV

^{67}Ga Citrate and ^{64}Cu Asparagine Distribution in Tumor Mice*
% dose/gram ± s.d.

	^{67}Ga Citrate		^{64}Cu Asparagine	
	3 hr (6)	24 hr (6)	3 hr (3)	20 hr (11)
Blood	27.10 ± 7.06	3.89 ± 2.09	4.75 ± 0.37	0.98 ± 0.21
Heart	5.98 ± 1.69	1.46 ± 0.70	2.28 ± 0.47	0.61 ± 0.17
Lungs	8.68 ± 1.59	3.47 ± 1.07	10.10 ± 3.33	1.48 ± 0.59
Liver	6.33 ± 1.40	9.56 ± 1.98	8.96 ± 1.11	20.40 ± 3.48
Kidneys	5.87 ± 0.92	5.56 ± 0.70	7.92 ± 0.45	3.08 ± 0.81
Spleen	6.81 ± 2.10	5.07 ± 1.37	2.19 ± 0.89	1.93 ± 0.30
Muscle†	0.97 ± 0.60	0.21 ± 0.15	0.61 ± 0.06	0.32 ± 0.31
Femur	2.88 ± 0.79	3.89 ± 0.38	1.63 ± 0.05	0.53 ± 0.39
Gut	4.45 ± 1.09	6.80 ± 1.74	2.34 ± 0.32	4.47 ± 2.27
Tumor	3.15 ± 0.73	3.96 ± 1.51	4.39 ± 0.45	2.30 ± 0.83
Carcass	2.52 ± 0.33	1.57 ± 0.23	1.08 ± 0.21	0.29 ± 0.07

* L-2 Lymphoma

† Muscle from femur

XBL7511-9151

Table V

^{67}Ga Citrate and ^{64}Cu Asparagine Distribution in Tumor Mice*
Ratio % dose/gram of tumor: % dose/gram of tissue ± s.d.

	^{67}Ga Citrate		^{64}Cu Asparagine	
	3 hr (6)	24 hr (6)	3 hr (3)	20 hr (11)
Blood	0.12 ± 0.02	1.39 ± 1.30	0.93 ± 0.16	2.27 ± 0.51
Heart	0.57 ± 0.24	3.49 ± 3.00	1.97 ± 0.38	3.91 ± 1.00
Lungs	0.37 ± 0.09	1.18 ± 0.55	0.48 ± 0.22	1.76 ± 0.74
Liver	0.52 ± 0.18	0.41 ± 0.15	0.50 ± 0.09	0.11 ± 0.03
Kidneys	0.54 ± 0.12	0.71 ± 0.28	0.56 ± 0.08	0.79 ± 0.30
Spleen	0.48 ± 0.08	0.78 ± 0.31	2.17 ± 0.06	1.12 ± 0.32
Muscle⁺	4.31 ± 2.57	31.70 ±29.90	7.22 ± 0.54	13.20 ±11.90
Femur	1.15 ± 0.29	1.01 ± 0.39	2.69 ± 0.31	6.47 ± 4.95
Gut	0.72 ± 0.12	0.65 ± 0.32	1.89 ± 0.08	0.50 ± 0.24
Carcass	1.27 ± 0.32	2.66 ± 1.16	4.14 ± 0.50	7.97 ± 2.99

* L-2 Lymphoma

⁺ Muscle from femur

XBL7511-9152

Figure Captions

Fig. 1. Compact rubidium-82 generator for obtaining multimillicurie amounts of ^{82}Rb with 2% NaCl.

Fig. 2. Stainless steel ion exchange column for easy connection to compact ^{82}Rb generator (Luer-Lock end fittings are not shown).

Fig. 3. Radiostrantium breakthrough for increasing volume of 2% NaCl elution of ^{82}Rb.

Fig. 4. Blood clearance of ^{62}Zn-histidine in a beagle dog from 0 to 70 min after i.v. administration of 200 μCi.

Fig. 5. Uptake of ^{62}Zn-histidine in a beagle dog 17 hr after i.v. administration of 200 μCi. Positron camera image shows uptake in prostate and colon. Six different intensities of the same image.

Fig. 6. Pancreas image of a monkey 1 hr after 700 μCi of ^{62}Zn-histidine with ^{99m}Tc sulfur colloid liver uptake subtracted by computer processing. The same technique was used with ^{75}Se selenomethionine as a comparison. Uptake in the heart is shown with the ^{75}Se image.

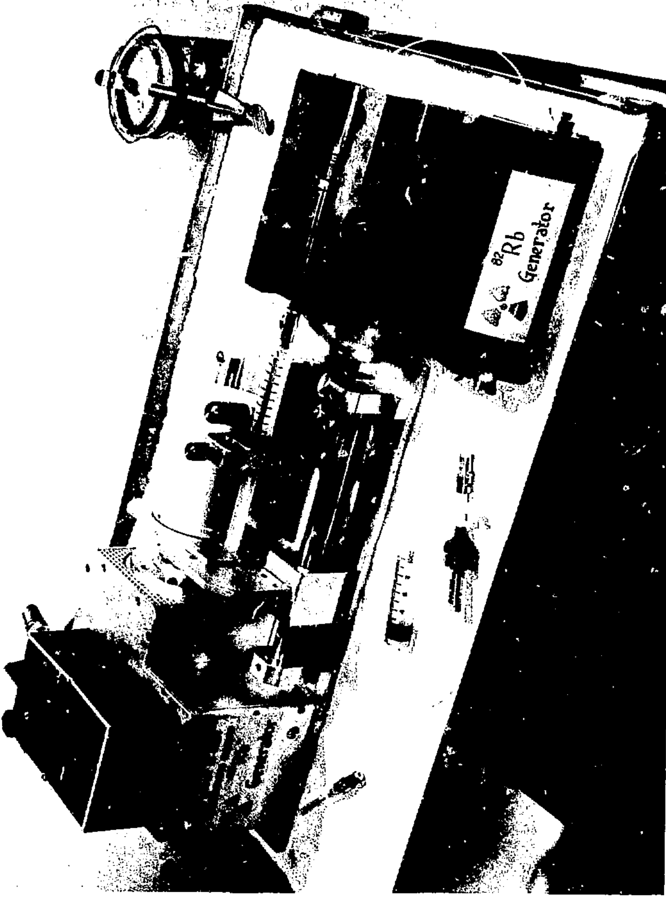

CBB 748-5258

Fig. 1

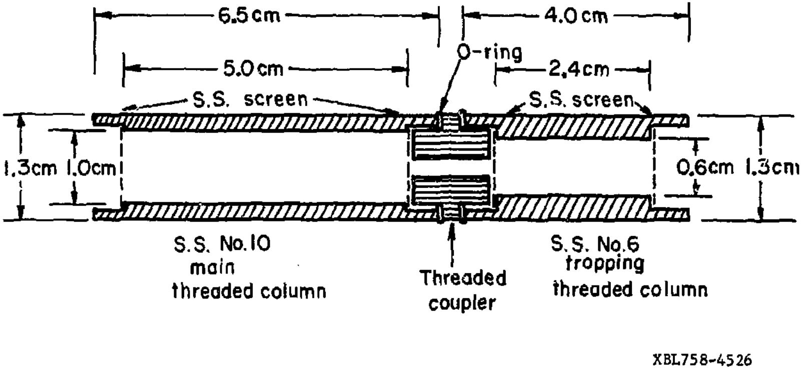
6.5cm
4.0cm
O-ring
5.0cm
2.4cm
S.S. screen
S.S. screen
1.3cm
1.0cm
0.6cm
1.3cm
S.S. No.10
main
threaded column
Threaded
coupler
S.S. No.6
tropping
threaded column
XBL758-4526

Fig. 2

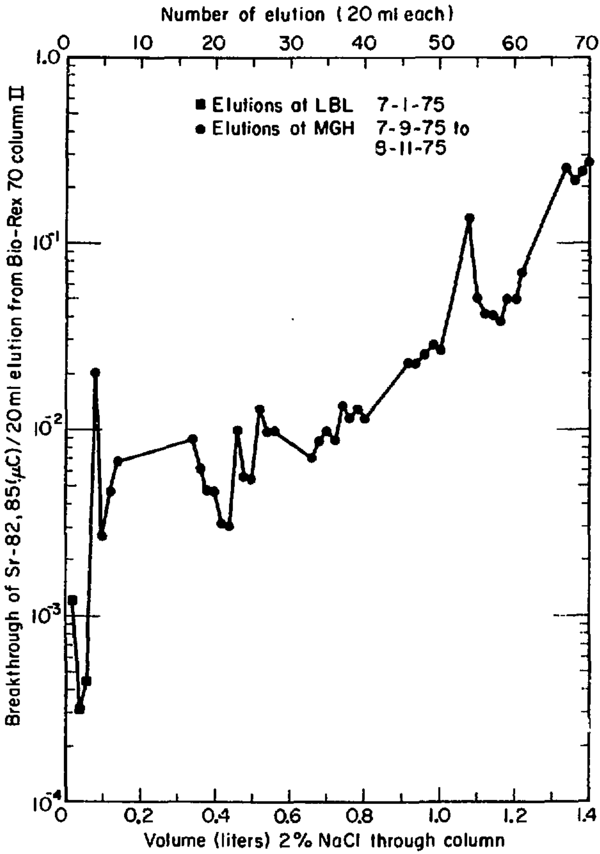

XBL761-5018

Fig. 3

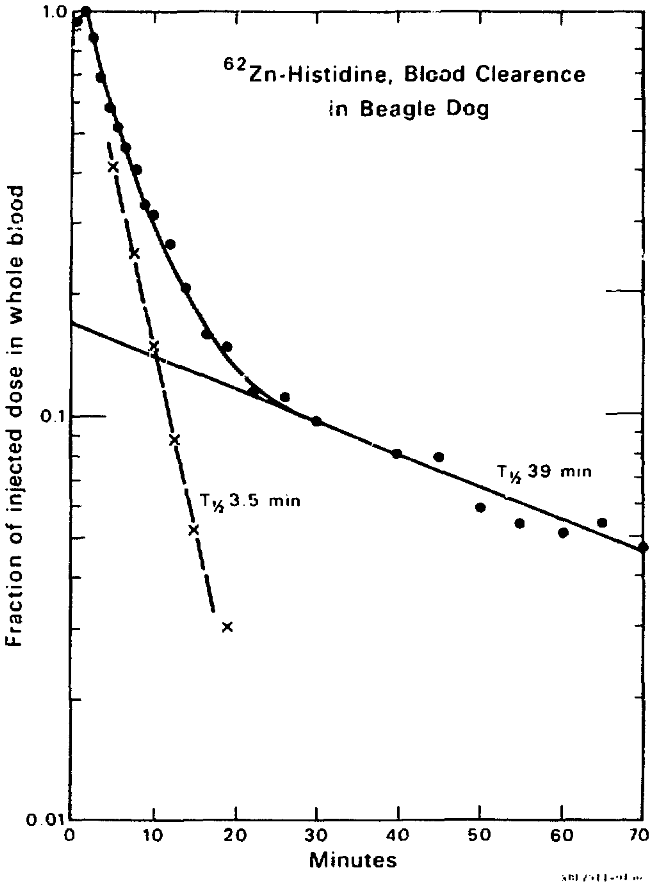

^{62}Zn-Histidine, Blood Clearence
in Beagle Dog
T½ 3.5 min
T½ 39 min
1.0
0.1
0.01
0
10
20
30
40
50
60
70
Minutes
Fraction of injected dose in whole blood

Fig. 4

^{62}Zn-Histidine, Dog at 17 hr

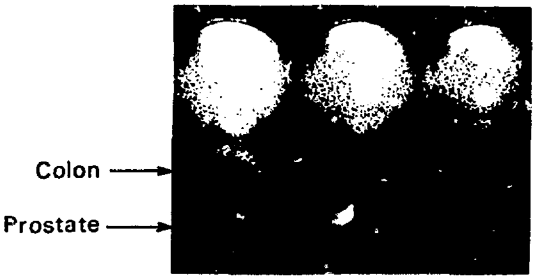

Anterior: Colon and Prostate

XBB 767-5939

Fig. 5

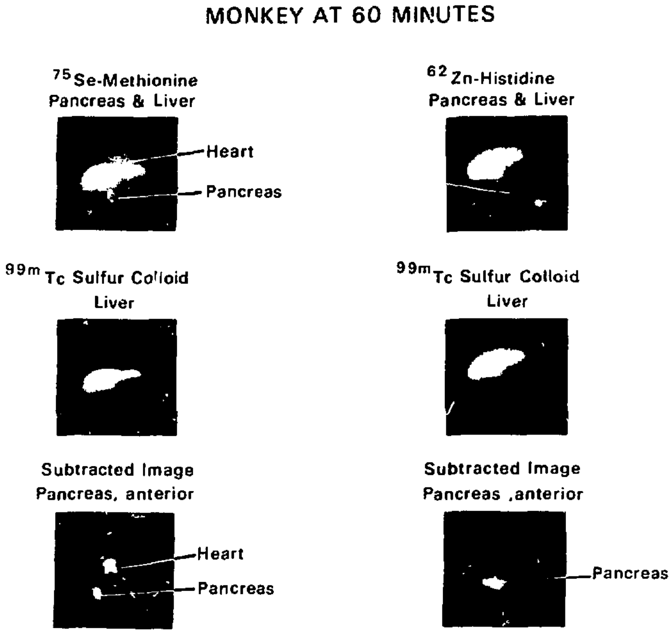

XBB 766-5431

Fig. 6